Chapter #

EXPERIMENTAL STUDY ON RSS BASED INDOOR POSITIONING ALGORITHMS

Hélder David Malheiro da Silva[1], José Augusto Afonso[2], and Luís Alexandre Rocha[3]

[1] *Centro Algoritmi, University of Minho, Guimarães, 4800-058, Portugal, e-mail: helderdavidms@gmail.com, phone: 351-253510180, fax: 351-253510189.*

[2] *Centro Algoritmi, University of Minho, Guimarães, 4800-058, Portugal, e-mail: jose.afonso@dei.uminho.pt, phone: 351-253510184, fax: 351-253510189.*

[3] *Centro Algoritmi, University of Minho, Guimarães, 4800-058, Portugal, e-mail: larocha@dei.uminho.pt, phone: 351-253510129 , fax: 351-253514400.*

Abstract: This work compares the performance of indoor positioning systems suitable for low power wireless sensor networks. The research goal is to study positioning techniques that are compatible with real-time positioning in wireless sensor networks, having low-power and low complexity as requirements. Map matching, approximate positioning (weighted centroid) and exact positioning algorithms (least squares) were tested and compared in a small predefined indoor environment. We found that, for our test scenario, weighted centroid algorithms provide better results than map matching. Least squares proved to be completely unreliable when using distances obtained by the one-slope propagation model. Major improvements in the positioning error were found when body influence was removed from the test scenario. The results show that the positioning error can be improved if the body effect in received signal strength is accounted for in the algorithms.

Keywords: Fingerprinting, linear least squares, localization, map matching, received signal strength, weighted centroid, wireless sensor networks.

1. INTRODUCTION

Localization capability in wireless sensor networks (WSN) brings spatial information to sensor data and enables numerous added value applications. Localization can be used in the most various contexts, from geodesic routing to antenna beam forming, or to detect soil temperature and pinpoint the origin of a wildfire.

In outdoors environment, the global positioning system (GPS) is capable of offering an adequate service to the majority of applications. Device size is no longer an issue in WSN due to the miniaturization of GPS hardware. Remaining disadvantages of this approach relate to energy consumption and node price when using this technology in WSN.

Regarding indoors environment, GPS is not reliable due to the signal attenuation. Ultra-wideband is a technology with potential to solve the problem of indoor location due to its high accuracy when inferring distances between devices [1]. However, and despite large standardization efforts (e.g., the IEEE 802.15.4a standard), a fully compliant commercial device for sale is unavailable. Since no mass market is currently in place, prices for available proprietary hardware are very high.

Received signal strength (RSS) based positioning is a popular approach in WSNs since RSS is readily available with the radio module. Due to typical WSN energy and computational profiles, low complexity positioning solutions are desired. As such, researchers seek to find balance between accuracy and computational complexity.

This work, which is a revised and extended version of our previous work [2], concerns the implementation of positioning systems (PS) in WSN that best fit the indoor scenario. We experimentally compare positioning calculation using map matching, approximate positioning and exact positioning algorithms in an indoor test scenario. We also study the effect of the body in the performance indicators.

Map matching solutions are mainly used in large areas, such as office settings and warehouses with several divisions. Our work differs from the usual approach, since the fingerprinting solution is implemented in a smaller predefined space of a room, without walls in between access points.

2. BACKGROUND

2.1 RSS Based Indoor Positioning Systems

An overview of technologies used in positioning systems is available in [3]. Ultrasound, ultra-wideband, radio-frequency identification (RFID) and RSS based systems are among the most used technologies for indoor

positioning. Accuracies span from 5 meters (RSS) to a few centimeters (ultrasound).

RSS systems are known for the low reliability when inferring distances from measurements. Filtering techniques are a solution for dealing with RSS reliability under noisy environment conditions. These techniques also stand as the common solution for integration of heterogeneous positioning systems, in order to provide more accurate location estimation. Kalman filters [4] and particle filters [5] are the usual approaches; however, since these solutions need high computational capacity, they are usually not compatible with WSNs. Instead, filtering is typically accomplished by averaging multiple measurements, thus positioning accuracy is sacrificed in the tradeoff for lower computational demands, longer lifespan of sensor nodes and faster positioning update rates when desired.

Propagation models are an important topic in RSS based systems, for which [6] presents a general overview. Several efforts have been made to characterize radio signal propagation [7], developing many propagation models. For indoor settings, the one-slope [8] and the multiwall [9] models are frequently used in state-of-the-art. Several types of fading affect these signals [10], where attenuations as high as 15 dBm are reported [11] due to the human body. We refer the reader to our previous work [2] for a more detailed description of this topic concerning the context of this work.

2.2 Map Matching

Two phases compose the system originally implemented by Bahl et al. [12]. In the offline phase, data relating position and RSS from access points (AP) is gathered from the site on to a database, in order to create a radio map. In the online phase, mobile nodes report to a server the RSS from APs in range. The server compares signatures so a match (or the closest to) can be found, thus pinpointing the mobile node's position.

In [13], a comprehensive study on fingerprinting is presented. Authors conclude that map density translates to higher accuracy with a nonlinear behavior in increasing the number of calibration points. The direction faced when collecting samples, also studied [12], is crucial and greatly improves system accuracy.

Approaches to facilitate creation of radio map in the offline phase have been conducted. Authors in [14] use propagation models to ease the process of creating the radio map. Ray-tracing modeling is another solution to obtain the attenuation values of signal propagation [15].

2.3 Approximate Positioning

The approximate positioning method uses parameters or metrics that can

be used to infer proximity to a known location. The weighted centroid localization (WCL) is a well-known approximate positioning method, which presents low complexity and good robustness to noise. Bulusu et al. implemented this method in [16], where node connectivity was the metric used to infer distance. Given a set of beacon nodes in the network possessing knowledge of their location, the position of sensor nodes can be estimated by calculating the centroid of all beacon node coordinates for which the sensor is in range of.

LANDMARC [17] uses RSS readings in their approximate positioning method. Tag readers report RSS from moving RFID tags, along with RSS from reference tags. Reference tags are fixed and their RSS is used as means of comparison between that of the movable tags to infer proximity. In a more recent work [18] authors further improve LANDMARC's positioning error to a 1-meter accuracy with a signal reporting cycle of 2 seconds.

Hop count positioning algorithms such as DV-Hop [19] can use RSS as a metric to infer distance for each hop. In [20], authors achieve less than 10 percent radio coverage error.

2.4 Exact Positioning

The exact positioning method involves the determination of angles or distances between a sensor node and multiple known reference points. Triangulation and trilateration (or multilateration) are the typical methods employed to determine the sensor position. Distance estimates are usually obtained by measuring the time of arrival (TOA), time difference of arrival (TDOA) or the round trip time of flight (RTOF) [21].

The linear least squares method (LLS) [22] is the most used exact positioning algorithm in WSNs, due to the simple closed form solution.

Measuring the propagation time of a transmission is a more robust method when compared to measuring the signal strength. However, in WSN this generally involves adding extra hardware, increasing energy consumption. The main goal in this work is the implementation of low power and real-time sensor node positioning in indoor environment. As such, addition of extra hardware is avoided and RSS measurements are performed for distance estimates.

3. MATERIALS AND METHODS

3.1 Hardware

Texas Instruments CC2530DK development kit was used in this work. We refer the readers to our previous work [2] for a more detailed description.

The test scenario is composed by four anchor nodes and one sensor node. Each anchor node is composed by a CC2530 evaluation module and a battery board powered by two AA batteries. The sensor node is composed by a development board and an evaluation module.

3.2 Experimental Setup

The anchor's role is to broadcast beacon messages periodically, so sensor nodes can receive these messages and locate themselves. Our main test bed is a room with 10×4.7 m free space area, as shown in fig. 1.

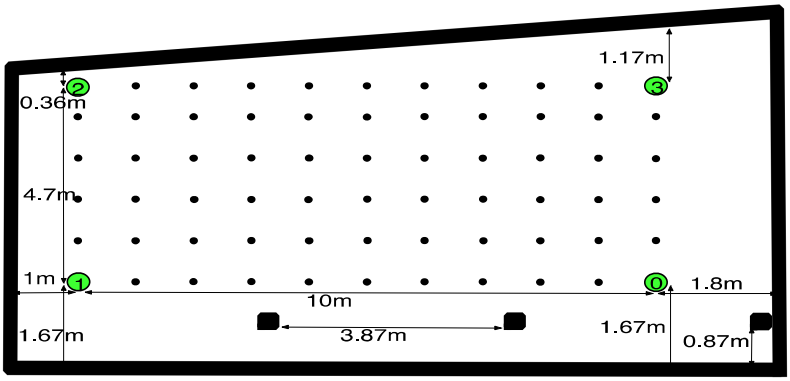

Fig. 1. Experimental setup. Anchor locations are depicted as green circles, along with distances to walls. Black dots indicate calibration points. A calibration point was also taken at each anchor location. The three supporting beams on the bottom right side of the figure are depicted as squares.

Anchors are placed in the corners of the mentioned area on top of a stand, 1.2 meters above ground. The stands used are made of plastic, so no extra interferences affect the radio messages.

Numbered from 0 to 3, each anchor broadcasts one beacon message periodically. Using the sequence number in the beacon messages, the sensor node detects lost beacons during data collection and inserts a value of -127, indicating an invalid RSS sample. Calculations are performed in an offline phase.

The one-slope propagation model used in this scenario was calibrated on site. Details on the calibration method used can be found in [2].

3.3 Map Matching

The radio map was created with a grid resolution of one squared meter. Since our positioning area is 4.7 meters wide, the last column of the grid has

a smaller resolution of 0.7 squared meters. A total of 66 grid points covered our test field. A calibration point was collected at each grid point and for each body orientation (e.g., north, west, south and east), amounting to a total of 264 calibration points. Each point is composed by true position (x and y with origin on anchor 0), body orientation and average RSS obtained from 100 RSS samples from all four anchor nodes.

During the online phase, the sensor node obtains and stores RSS samples. At the end of a test run (e.g.: after collecting 100 samples), data is uploaded to a PC running MATLAB and the position is computed. The weighted k-nearest neighbor (WKNN) algorithm [12] uses (1) to find the distance in signal space between a RSS sample and each calibration point.

$$D_{SS} = \left[\sum_{i=1}^{N} \left| R_{map}(i) - R_s(i) \right|^p \right]^{\frac{1}{p}} \quad (1)$$

N is the number of anchor nodes in range and p is the norm used. The $R_{map(i)}$ is the RSS stored for anchor i in a calibration point of the radio map and $R_s(i)$ is the RSS sampled in the online phase for anchor i. After computing the distances for all calibration points, the K smallest distances are used to estimate the node's position using (2), where p_i is the coordinates of each calibration point.

$$\hat{x} = \frac{\sum_{i=1}^{K} w_i \times \vec{p}_i}{\sum_{i=1}^{K} w_i}; \; w_i = \frac{1}{D_1} \quad (2)$$

The weight applied to each neighbor found in the search process is simply the inverse of the signal space distance.

3.4 Approximate Positioning

In this type of positioning, the only information needed by a node to calculate its position is the coordinates of each anchor node in range. The position estimate is calculated using (3):

$$\hat{x} = \frac{\sum_{i=1}^{B} w_i \times \vec{L}_i}{\sum_{i=1}^{B} w_i}; \; w_i = \left| \frac{1}{(R_p)^e} \right| \quad (3)$$

Where L_i is the coordinates of each anchor node and R_p is the radio parameter used to calculate the weight. In this work, both the RSS and the distance using a propagation model were used to calculate the weights, in two different approaches. The exponent e allows an adjustment of the importance of the weight applied to each anchor node's RSS.

3.5 Exact Positioning

The Linear Least Squares method is an exact positioning technique, which computes the position of a node using a set of three or more non-collinear distance measurements (in the two dimensional case). Each measurement produces an equation of the form illustrated in (4):

$$(x - x_n)^2 + (y - y_n)^2 = d_n^2 \tag{4}$$

Several measurements produce a system of equations, which has no solution when circles don't intersect. To find a solution to this system, first a linearization of the system of equations is obtained by subtracting the location of the first anchor node from other locations. This cancels the unknown squared terms, and a linear system of the form **Av** = **b** is obtained, as shown in (5), (6) and (7):

$$\mathbf{A} = 2 \times \begin{pmatrix} x_1 - x_2 & y_1 - y_2 \\ x_1 - x_3 & y_1 - y_3 \\ \cdots & \cdots \\ x_1 - x_n & y_1 - y_n \end{pmatrix} \tag{5}$$

$$\mathbf{b} = \begin{pmatrix} d_2^2 - d_1^2 + x_1^2 - x_2^2 + y_1^2 - y_2^2 \\ d_3^2 - d_1^2 + x_1^2 - x_3^2 + y_1^2 - y_3^2 \\ \cdots \\ d_n^2 - d_1^2 + x_1^2 - x_n^2 + y_1^2 - y_n^2 \end{pmatrix} \tag{6}$$

$$\mathbf{v} = \begin{pmatrix} x \\ y \end{pmatrix} \tag{7}$$

Since the vector **b** may be located outside the plane defined by matrix **A**, the solution is to find the projection of **b** onto **A**, thus minimizing the Euclidean distance (or squared error), using (8).

$$\mathbf{v} = (\mathbf{A}^{\mathbf{T}} \times \mathbf{A})^{-1} \times (\mathbf{A}^{\mathbf{T}} \times \mathbf{b}) \tag{8}$$

4. RESULTS

Two sets of samples were collected, with one set being obtained with the user's body near the receiving antenna (BP set), the other set without the body influence (BNP set). A set is composed by several test runs; each test run contains 100 RSS samples. Position estimation is computed for each sample in a test run, thus no averaging was used in the results presented.

All sample sets were taken in positions where a calibration point exists. The BP set is composed by 79 test runs, from which 66 were taken facing the north direction. The remaining 13 test runs were randomly chosen across the positioning area, with different orientations. The BNP set is composed by 12 test runs randomly chosen and do not have an orientation associated since the body is not present.

The height of the sensor nodes is the same as the anchor nodes (1.2 meters above ground). The mean error (ME) and standard deviation (STD) of the absolute error (Euclidean distance between the calculated position and the true position) were the metrics chosen as primary performance indicators.

4.1 Map Matching

The radio map is a representation of the propagation conditions that the algorithms were subject to. Fig. 2 illustrates the average RSS for each of the anchor nodes obtained from all calibration points.

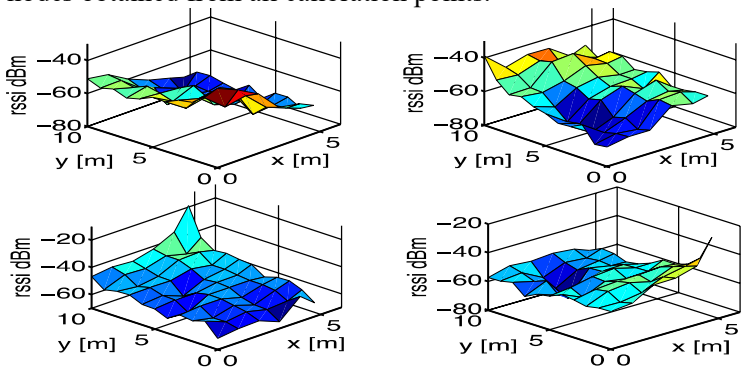

Fig. 2. Average RSS fingerprint map. Top left: anchor 0; top right: anchor 1, bottom left: anchor 2 and bottom right: anchor 3.

The RSS values from fig. 2 were obtained by averaging all calibration points in a given x and y position for all four directions. The values depicted clearly correlate with the position of the anchor nodes, where the strongest RSS values appear in the area where the anchor is located.

Two parameters were tested in the map matching solution: the number of neighbors K and the norm used p. The ME and STD are presented in fig. 3.

The body influence is presented for each of the p-norms tested. In the BP case, the ME variation between K=1, equivalent to nearest neighbor (NN) algorithm, and the other values of K is not significant. This can be explained due to the positioning system area and calibration point density. Since the area is small and the density of calibration points is high, the NN algorithm tends to perform as good as WKNN. Other works, such as [13], also pointed out this outcome, yet under a different environment. Note that a map matching solution with NN as the positioning algorithm only needs to find

one nearest neighbor, which is computationally faster than the WKNN case.

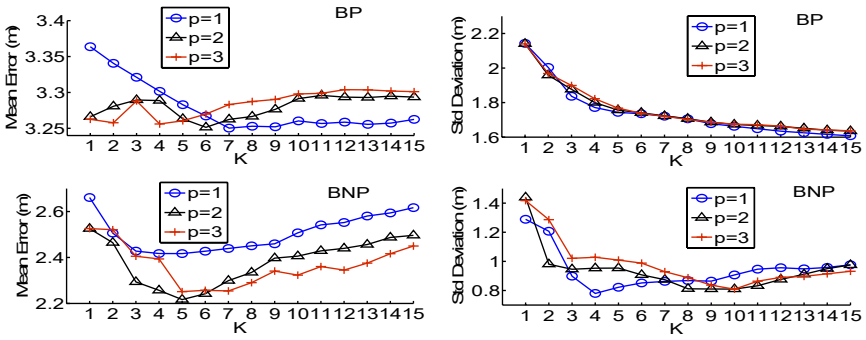

Fig. 3. ME (left side) and STD (right side) for different values of K and p. At the top is displayed the BP case, at the bottom is displayed the BNP case.

In the BNP case, the value K has a more important influence than in the BP case, where for p=2 and K=5, ME reaches a minimum of approximately 2.2 meters. This scenario where body influence is not present is, of course, a best-case scenario, which does not happen when the system is to be used by a person. Yet, it shows a boundary of positioning error that deterministic frameworks can provide in this environment, if accounting the body influence in the position calculation.

The STD values exhibit a monotonic decrease, with the increase of K in the BP case. Differences between norms are negligible. In the BNP case, STD values reach a minimum of 0.8 meters for p=1 and K=4.

4.2 Approximate Positioning

RSS (RWCL) and distance using the one-slope path loss model (DWCL) are tested as weights in the WCL algorithm. In the RWCL, the exponent e was varied. Results are presented in fig. 4.

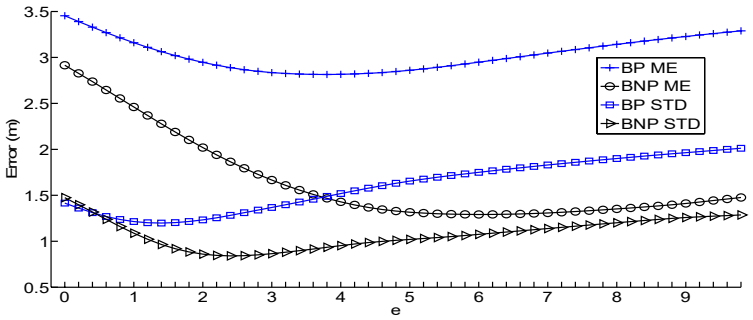

Fig. 4. ME and STD for different values of exponent e, for both BP and BNP case.

In contrast with other works [23], [24], we found the optimum e parameter

between 2 (BP) to 6 (BNP), where a tradeoff between the ME and STD exists. As the parameter *e* increases beyond 4 in the BP case, and beyond 6 in the BNP case, ME and STD also increase. With a high *e* value, the position is strongly influenced by the anchor node with the greater RSS reading. In limit conditions, the calculated position would be the same as that of the anchor node with higher RSS in the field. Again, body influence plays a very important role. As an example, for an exponent of *e*=4, the ME in the BNP case is approximately half of the ME in the BP case. In the case of STD, an improvement of more than 50% in the BNP case is also achieved.

In the DWCL algorithm, two parameters can be varied: exponent *e* and the path loss exponent *n*. Results are presented in fig. 5.

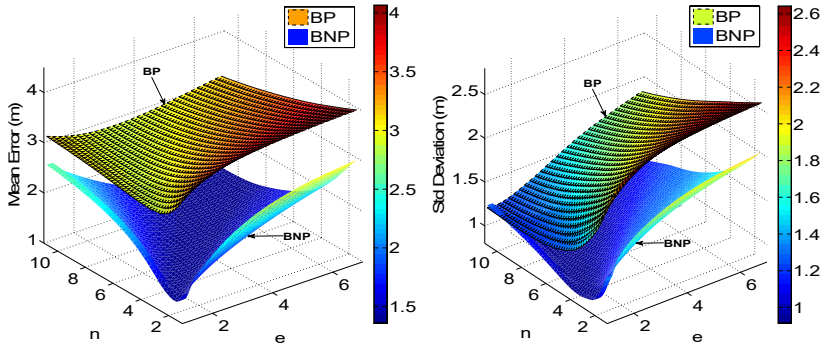

Fig. 5. DWCL ME (left side) and STD (right side) for different values of path loss exponent n and parameter e.

The minimum ME of 1.36 meters is achieved (*n*=2.2, *e*=1.4) in the BNP case, while in the BP case, minimum ME was 2.92 meters (*n*=3.4, *e*=1). Body influence increases the error by a factor slightly higher than 2.

There is a balance between parameters, due to *n* and *e* balancing each other, which can be seen as the "saddle" effect in fig. 5.

The value of *n*=2.2 obtained in the BNP case is also very similar to the value obtained in [2] of *n*=2.19, which validates the use of linear regression as an appropriate method of determining path loss exponent when in LOS conditions.

4.3 Exact Positioning

The influence of the parameter *n* of the one-slope model, used in the RSS to distance conversion, was tested. Results for the LLS algorithm are depicted in fig. 6.

Increasing the value of *n* produces a dampening effect on the error, since the estimated circumferences around each anchor node become smaller. Even though the ME and the STD decrease as *n* increases, the algorithm exhibits a saturated behavior, has can be seen for values of *n* higher than 6.

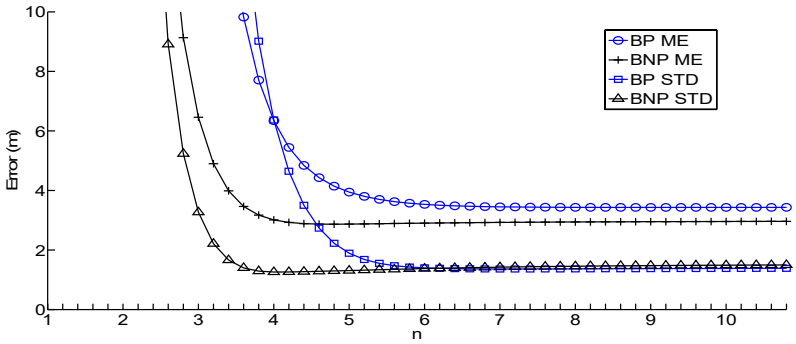

Fig. 6. LLS ME and STD for different values of path loss exponent n.

Positioning error increases rapidly for values of n smaller than 4. For a value of n=2.19, as obtained for the one-slope model used in this work, the ME rises to around 1000 meters, many orders higher than the positioning area itself, which renders the algorithm useless.

4.4 Algorithm Comparison

For the algorithm comparison, the best parameter values for each of the algorithms were considered. To have a frame of reference, a fictitious positioning algorithm, called static center position (SCP) was added to each CDF plot. This algorithm simply returns the center position of the PS area, for any input. The CDF plots for WKNN (k=5 p=2 for BNP case, k=1 p=2 for BP case) and LLS (n=6 for BNP case, n=9 for BP case) algorithms; RWCL (e=6 for BNP case, e=3.4 for BP case) and DWCL (n=2.2 e=1.4 for BNP case, n=3.4 e=1 for BP case) are presented in fig. 7.

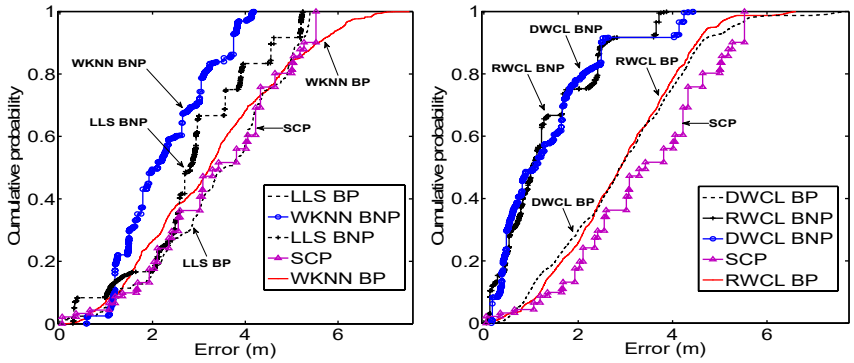

Fig. 7. Cumulative Distribution Functions for WKNN and LLS algorithms (left side), RWCL and DWCL algorithms (right side).

Regarding the WKNN algorithm, the body influence is evident, with a 30 percent improvement for an error of 3 meters. The body has a bigger impact

on WCL than in the map matching solution, yet the WCL algorithms present slightly better results than WKNN when under body influence. When body is not present, WCL produces the best position estimates of all algorithms tested. Considering a probability of around 70 percent, WCL improves from an accuracy of 4 meters (BP case) to approximately 1.8 meters (BNP case).

RWCL and DWCL obtained equivalent performances, which implies that RSS is the best weighting solution in WCL for our setup, since it is simpler than using a propagation model.

LLS had the worst performance, where the BNP case performed at the same level of the BP case for the other algorithms. When compared with SCP, LLS can even sometimes perform worse.

4.5 Body Influence On RSS

We collected two sets of measurements inside an anechoic chamber. These measurements were obtained by placing an anchor node and a sensor node two meters apart. In the first set of measurements, which we will call static mode, the node is placed on top of a plastic stand and there is no body influence; in the second set of measurements, which we will call dynamic mode, the node is attached to the user's body.

In the static mode, several readings are obtained in different sensor node orientations (approximately 15 degrees between readings). In the dynamic mode, the user performs a 360-degree turn for approximately 60 seconds. The module of the RSS values for both modes is presented in fig. 8.

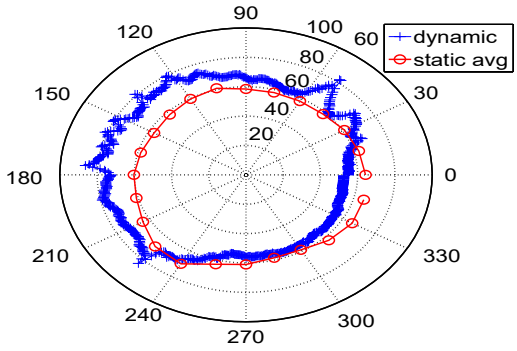

Fig. 8. Module of RSS values obtained inside the anechoic chamber.

The user is facing the anchor node in the 0-degree direction. From fig. 8, despite the attenuation peaks that occurred between 30 and 60 degrees, we can see there is a trend in the mean value of the dynamic mode. Mean attenuation value rises when the user rotates past the 90-degree direction and until 180 degrees. Mean attenuation decreases between 180 and 270 degrees, point from which the mean value starts to exhibit the same trend as in the 0-degree direction.

5. DISCUSSION

Propagation models typically model large-scale fading LOS propagation. Body influence, NLOS between nodes and multipath dominated environments induce large variations in RSS, which are not accounted for in the propagation model. The comparison between the results obtained for the BP and BNP case demonstrate how strong the body influence is. Also, measurements obtained in the anechoic chamber also suggest that body influence is important when estimating the position using RSS.

The use of propagation models proved to be unreliable in the case of the LLS algorithm. Distances estimated by the propagation model used as weights in approximate positioning algorithms produced acceptable results, yet they did not surpass results using RSS alone as weight.

Although more information from the propagation environment is embedded in the map matching solution, which includes body orientations, the results obtained did not compensate such effort when compared to WCL algorithm. Approximately two hours were needed to collect all calibration points in our small test environment. If a bigger area were involved, the offline phase map creation would be harder to accomplish without resorting to other mapping techniques.

In the BP case, performance obtained from the WCL solutions is equivalent to the map matching solution. WCL solutions provided the best position estimates in the BNP case. This, associated with the fact that RWCL solution does not require prior calibration and setup, makes this type of positioning the best possible under our test conditions.

The LLS based on propagation model solution provided the weakest results. Clearly, LLS algorithm cannot be used with RSS measurements in such an environment. LLS algorithm needs more accurate methods to detect distance between nodes.

6. CONCLUSIONS AND FUTURE WORK

From the results obtained we can conclude that the RWCL solution provides overall better results than map matching, with the advantage of having lower complexity and easier setup. The LLS is an inappropriate solution when using RSS to estimate position in indoor environment. Distances estimated from propagation models are severely affected by biases that heavily depend on factors such as body orientation, LOS/NLOS condition, multipath between nodes and proximity to other objects, walls or obstructions. Approximate positioning algorithms tend to perform better in this kind of environment due to its error resilience.

All algorithms showed poor positioning capabilities when body influence

is present. When body influence is removed, positioning accuracy improves drastically, with the exception of LLS. Between all three types of positioning algorithms, body influence impact was small in the LLS case, medium in the map matching solution, and highest in the WCL algorithms.

Anchor node placement is a very important issue in RSS positioning systems that has not been addressed in this work. A minimum number of anchor nodes were employed, assuring always a total of four non-collinear points. Increasing the number of anchor nodes in the test area is another possibility to further reduce positioning error. This measure needs to be taken with caution in the case of WKNN, since increasing number of anchor nodes also increases algorithm complexity.

As future work, we intend to integrate the RSS indoor positioning capability in our wireless posture monitoring system (WPMS) [25]. The WPMS is a motion capture system that uses information from multiple inertial and magnetic sensors placed in the user's body. The objective is to provide location information, which, together with the body posture, will characterize not only how the user is moving but also his location.

ACKNOWLEDGMENT

Helder D. Silva is supported by the Portuguese Foundation for Science and Technology under the grant SFRBD/78018/2011.

REFERENCES

1. E. Karapistoli, F.-N. Pavlidou, I. Gragopoulos, and I. Tsetsinas, "An overview of the IEEE 802.15.4a Standard," IEEE Commun. Mag., vol. 48, no. 1, pp. 47–53, Jan. 2010.
2. H. D. Silva, J. A. Afonso and L. A. Rocha, Experimental Performance Comparison of Indoor Positioning Algorithms based on Received Signal Strength, Lecture Notes in Engineering and Computer Science: Proceedings of The World Congress on Engineering 2014, WCE 2014, 2-4 July, 2014, London, U.K., pp.677 -683.
3. T. K. Kohoutek, R. Mautz, and A. Donaubauer, "Real-time Indoor Positioning Using Range Imaging Sensors," in Proceedings of SPIE Photonics, 2010, vol. 7724, no. May, p. 77240K–77240K–8.
4. G. Glanzer, T. Bernoulli, T. Wiessflecker, and U. Walder, "Semi-autonomous indoor positioning using MEMS-based inertial measurement units and building information," 2009 6th Work. Positioning, Navig. Commun., vol. 2009, pp. 135–139, Mar. 2009.
5. H. Wang, H. Lenz, A. Szabo, J. Bamberger, and U. D. Hanebeck, "WLAN-Based Pedestrian Tracking Using Particle Filters and Low-Cost MEMS Sensors," 2007 4th Work. Positioning, Navig. Commun., vol. 2007, pp. 1–7, Mar. 2007.
6. I. Forkel and M. Salzmann, "Radio Propagation Modelling and its Application for 3G Mobile Network Simulation," 10th Aachen Symp. Signal Theory, pp. 363–375, 2001.
7. E. Damosso and L. M. Correia, Cost 231 Final Report: Digital Mobile Radio Towards Future Generation Systems. 1999.
8. Z. Zhang, G. Wan, M. Jiang, and G. Yang, "Research of an adjacent correction positioning algorithm based on RSSI-distance measurement," 2011 Eighth Int. Conf. Fuzzy Syst. Knowl. Discov., pp. 2319–2323, Jul. 2011.

9. S.-Y. Yeong, W. Al-Salihy, and T.-C. Wan, "Indoor WLAN Monitoring and Planning Using Empirical and Theoretical Propagation Models," 2010 Second Int. Conf. Netw. Appl. Protoc. Serv., pp. 165–169, Sep. 2010.
10. T. S. Rappaport, Wireless Communications: Principles and Practice. Englewood Cliffs, New Jersey: Prentice-Hall, 1996.
11. E. Miluzzo, X. Zheng, K. Fodor, and A. T. Campbell, "Radio Characterization of 802.15.4 and Its Impact on the Design of Mobile Sensor Networks," in 5th European Conf. on Wireless Sensor Networks (EWSN '08), 2008, pp. 171–188.
12. P. Bahl and V. N. Padmanabhan, "RADAR: An in-building RF-based user location and tracking system," in INFOCOM 2000. Nineteenth Annual Joint Conference of the IEEE Computer and Communications Societies. Proceedings. IEEE, 2000, vol. 2, pp. 775 – 784 vol.2.
13. V. Honkavirta, T. Perala, S. Ali-Loytty, and R. Piche, "A comparative survey of WLAN location fingerprinting methods," in 2009 6th Workshop on Positioning, Navigation and Communication, 2009, vol. 2009, pp. 243–251.
14. P. Mestre, L. Coutinho, L. Reigoto, J. Matias, and C. Serodio, "Hybrid technique for Fingerprinting using IEEE802 . 11 Wireless Networks," in International Conference on Indoor Positioning and Indoor Navigation, 2011, no. September.
15. A. V. Bosisio and C. N. R. Ieiit, "Performances of an RSSI-based positioning and tracking algorithm," in International Conference on Indoor Positioning and Indoor Navigation, 2011, no. September.
16. N. Bulusu, J. Heidemann, and D. Estrin, "GPS-less low-cost outdoor localization for very small devices," Pers. Commun. IEEE, vol. 7, no. 5, pp. 28–34, 2000.
17. L. M. Ni, Y. Liu, Y. C. Lau, and A. P. Patil, "LANDMARC: Indoor Location Sensing Using Active RFID," Wirel. Networks, vol. 10, no. 6, pp. 701–710, Nov. 2004.
18. X. Yinggang, K. JiaoLi, W. ZhiLiang, and Z. Shanshan, "Indoor location technology and its applications base on improved LANDMARC algorithm," 2011 Chinese Control Decis. Conf., no. 2, pp. 2453–2458, May 2011.
19. S. Tian, X. Zhang, P. Liu, P. Sun, and X. Wang, "A RSSI-Based DV-Hop Algorithm for Wireless Sensor Networks," 2007 Int. Conf. Wirel. Commun. Netw. Mob. Comput., pp. 2555–2558, Sep. 2007.
20. R. Nagpal, H. Shrobe, and J. Bachrach, "Organizing a Global Coordinate System from Local Information on an Ad Hoc Sensor Network," in Proceedings of the 2nd international conference on Information processing in sensor networks, 2003, pp. 333–348.
21. J. Hightower and G. Borriello, "A Survey and Taxonomy of Location Systems for Ubiquitous Computing," 2001.
22. A. Savvides, C.-C. Han, and M. B. Strivastava, "Dynamic fine-grained localization in Ad-Hoc networks of sensors," Proc. 7th Annu. Int. Conf. Mob. Comput. Netw. - MobiCom '01, pp. 166–179, 2001.
23. J. Blumenthal, R. Grossmann, F. Golatowski, and D. Timmermann, "Weighted Centroid Localization in Zigbee-based Sensor Networks," 2007 IEEE Int. Symp. Intell. Signal Process., pp. 1–6, 2007.
24. F. Reichenbach and D. Timmermann, "Indoor Localization with Low Complexity in Wireless Sensor Networks," 2006 IEEE Int. Conf. Ind. Informatics, pp. 1018–1023, Aug. 2006.
25. H. D. Silva, P. Macedo, J. A. Afonso, and L. A. Rocha, "Design and implementation of a wireless sensor network applied to motion capture," *1st Portuguese Conference on Wireless Sensor Networks (CNRS 2011)*, Coimbra, Portugal, 2011.